

A genetically encodable cell type specific protein synthesis inhibitor (gePSI)

Maximilian Heumüller^{1,2}, Caspar Glock^{1,2}, Vidhya Rangaraju¹, Anne Bieber¹, and Erin
M. Schuman^{1,*}

¹ Max Planck Institute for Brain Research, Frankfurt am Main, Germany

² Contributed equally

* to whom correspondence should be addressed: erin.schuman@brain.mpg.de

Text added or altered in this revised manuscript is highlighted.

This version of the article has been accepted for publication, after peer review and is subject to Springer Nature's [AM terms of use](#), but is not the Version of Record and does not reflect post-acceptance improvements, or any corrections. The Version of Record is available online at: <https://doi.org/10.1038/s41592-019-0468-x>

Abstract

The changes in protein synthesis that drive cellular plasticity have largely been discovered via the introduction of chemical inhibitors that interfere with protein synthesis in all cells. Here we have developed a genetically encodable protein synthesis inhibitor (gePSI) that can be combined with common genetic targeting systems to achieve cell type- and temporally-specific control of protein synthesis. Controlled expression of the gePSI in neurons (or glia) resulted in rapid inhibition of protein synthesis that recovered over time. Moreover, gePSI expression in a single neuron blocked the structural spine plasticity induced by single synapse stimulation.

Main

Proteins are the main functional unit within cells that control biological processes. In all cells, protein synthesis is used to respond to extra- and intracellular cues to remodel cellular function. In the brain protein synthesis is crucial for some forms and specific temporal phases of synaptic plasticity¹. All studies probing the role of protein synthesis have used chemical inhibitors, often common antibiotics, which are effective but lack functional and cell type specificity. Here we developed a fully genetically encodable protein synthesis inhibitor (gePSI) that allows one to control protein synthesis in a temporal and spatial manner.

To develop a gePSI we considered the class of bacterial and plant toxins from the Shiga and Ricin families that are known as “ribosome inactivating proteins” (RIPs)^{2,3}; most RIPs effect a complete shutdown of protein synthesis by **depurinating adenine-4324 on the sarcin/ricin-loop** of the 28s rRNA⁴ (Fig. 1a). Specifically, we used an atypical class-I RIP from maize (*Zea mays*)^{5,6}. The full-length maize RIP contains two catalytically active chains as well as inactivation regions, which are proteolytically eliminated during RIP activation to increase enzyme potency. In order to induce the expression of various gePSI candidates in **hippocampal cultures** we used the TetOn3G system in which doxycycline (dox) introduction enables expression (Fig. 1b, c and S1a). We measured the efficacy of different candidate gePSIs by metabolic labeling of transfected cultured hippocampal neurons with a brief pulse of puromycin, followed by detection of nascent protein *in situ*⁷. The synthetic ProRIP molecule contains the active chains as well as a single internal inactivation region (Fig. 1c, (i)). The mere co-transfection of ProRIP (**pCMV-Tet3G + pTRE3G-ProRIP + pCMV-AcGFP**) into neurons in the absence of dox induction resulted in complete shutdown of protein synthesis in a majority of the cells (Fig. 1d, f). **We reasoned that the potency of the ProRIP in combination with leakiness of the TetOn3G system could be sufficient to inhibit protein synthesis. Thus, we physically separated the two chains (labelled “alpha and beta”, Fig. 1c) of the ProRIP to decrease the likelihood of leaky induction of both components.** We co-transfected neurons with a plasmid containing both chains driven by a bi-directional dox-inducible promoter as well as the activator plasmid (Fig. 1c, (ii); Fig. S1a). Using this strategy, protein synthesis levels in transfected but uninduced neurons (“no dox”) were indistinguishable from control, untransfected neurons (Fig. 1e, g). In contrast, a 4 hr induction resulted in a dramatic and uniform reduction of protein synthesis in transfected, but not

neighboring untransfected, neurons (Fig. 1e, g). The inhibition of protein synthesis required the combined expression of the alpha and beta chains, as expression of either chain alone did not inhibit protein synthesis (Fig. S1b-e). The gePSI-induced inhibition of protein synthesis was also detected with an alternative metabolic labeling approach that uses non-canonical amino acids^{8,9} (Fig. S2a, b) and was indistinguishable from that observed following treatment with the chemical protein synthesis inhibitor anisomycin (Fig. S2c, d). Moreover, expression of the gePSI did not promote cell death even when continuously expressed for 6 days (Fig. S3a-d), indicating that it can be used to perturb protein synthesis without obvious adverse effects on cellular health.

The time scales over which protein synthesis influences cellular and neuronal plasticity range from minutes to days^{1,10}. To determine the temporal precision of the protein synthesis inhibition driven by the gePSI, we varied the duration of the expression induction by dox from 0.5 to 4 hrs (Fig. 2a). In the last 10 min of the dox induction we measured protein synthesis, as before. Inducing the expression of the gePSI for less than 1 hr did not result in a consistent inhibition of protein synthesis in hippocampal neurons (Fig. 2a). Inducing for 2 or 4 hrs, however, resulted in a consistent and complete inhibition of neuronal protein synthesis (Fig. 2a). The observed requirement for at least 2 hrs of induction could represent the time needed to achieve adequate levels of the gePSI mRNA or the time needed for the gePSI protein to express. To distinguish between these possibilities, we induced with dox for variable durations but then delayed the measurement of protein synthesis to a uniform end point of 4 hrs following the initiation of induction (Fig. 2b). This experiment revealed that even a 30 min induction of the gePSI transcription was sufficient to significantly reduce protein synthesis measured 3.5 hrs later (Fig. 2b) although the inhibition of protein synthesis exhibited even greater reliability with longer induction periods (Fig. 2b).

In many *in vitro* and *in vivo* experiments, plasticity is induced by a brief external event that results in a defined period of protein synthesis that is required for the plasticity expression^{11,12}. To determine whether we could effect a temporally discrete period of protein synthesis inhibition that later exhibits recovery, we first optimized the dox concentration (Fig. S4a), induced the gePSI and then examined protein synthesis in neurons at 4, 24, 48 and 72 hrs (Fig. 2c, d). As before, protein synthesis was

inhibited following 4 hrs of gePSI induction (Fig. 2c, d). Probing 24 hrs later, however, revealed a significant recovery of protein synthesis levels in a large proportion of neurons, which increased over time to almost 90% recovery after 72h. In order to address why some neurons did not recover we quantified gePSI expression using fluorescence *in situ* hybridization, reasoning that enhanced persistence or levels of gePSI expression might lead to prolonged recovery times (Fig. S4b, c). Indeed we found that neurons which did not show recovery after 24h exhibited higher gePSI mRNA levels when compared to fully recovered neurons. We noted that those neurons that exhibited retarded recovery within the timecourse measured, however, did not exhibit enhanced apoptosis when probed 24/48 hrs after a 4 hr gePSI induction (Fig. S4d, e). These data indicate that the gePSI can transiently inhibit protein synthesis in cells for a defined period of time; these cells then exhibit functional recovery of their protein synthesis capabilities.

The ideal gePSI should exhibit spatial (e.g. cell type-specific) as well as temporal control. The simplest implementation of a cell type-specific gePSI could involve the use of a cell type-specific promoter to drive gePSI expression (Fig. 1b), for example in Camk2a-positive (Fig. S5a, c), GFAP-positive (Fig. S5b, d) cells or other cell lines (Fig. S5e-f). To maximize flexibility, we combined the platform with a Cre-inducible system (Fig S6a). To include temporal control, we floxed an HA (epitope)-tagged Tet3G (activator) element to enable Cre-induction, either via an external construct, or via introduction to a transgenic animal line. The Cre-dependent expression of Tet3G together with the addition of dox provides cell type-specificity and temporal control, respectively. We transfected neurons with the floxed Tet3G, the gePSI and a Cre recombinase plasmid. Only those cells that expressed Cre and were treated with dox exhibited significantly reduced protein synthesis (Fig. S6b, c). These data indicate that the gePSI can be used to bring about a temporally discrete episode of protein synthesis inhibition in an identified cell type (Fig. S6d, e).

Although some short-term forms of synaptic plasticity rely exclusively on covalent modifications of pre-existing proteins, many forms of plasticity, both synaptic and behavioral, require protein synthesis^{1,13}. To test the function of the gePSI during plasticity we first examined the compatibility of gePSI expression with synaptic transmission. We expressed the Ca²⁺-indicator GCaMP6s in cultured hippocampal neurons and determined their ability to respond to extracellular stimulation, using

two-photon (2P) uncaging of caged glutamate (Fig. 3a-c). gePSI-expressing neurons were competent to respond to single stimuli of individual dendritic spines as well as trains of stimulation (Fig. 3a-c). Using 2P glutamate uncaging, we induced a form of plasticity that is known to require protein synthesis¹² (Fig. 3d). This plasticity results in an enlargement of the stimulated spine, which is associated with enhanced synaptic responsiveness. Single spine stimulation (0.5 Hz) in neurons transfected with the gePSI in the absence of dox exhibited a rapid and persistent (~ for up to 55 min) increase in spine-head volume (Fig. 3d, e). Similarly, neurons that expressed Tet3G but not the gePSI also exhibited the stimulation-induced plasticity. However, neurons that expressed the gePSI in the presence of dox exhibited only a small increase in spine-head volume immediately after stimulation that decayed back to baseline values within 10 mins or so, indicating a requirement for protein synthesis in the stimulated neuron.

Here we have developed a genetically encodable protein synthesis inhibitor that can be induced to effectively, rapidly (e.g. within a few hours), and reversibly shutdown protein synthesis in targeted cells; neighboring cells are unaffected. By judicious use of both Cre-targeting and temporal induction, neurons that project to specific areas could be targeted for inhibition *in vivo* to probe the importance of different cell populations in learning and memory. In addition, the cell type-specific inhibition we achieve suggests that the gePSI could be used clinically to target identifiable cell populations, e.g. rapidly proliferating cells, to abbreviate cancer states.

References

1. Sutton, M. A. & Schuman, E. M. Dendritic protein synthesis, synaptic plasticity, and memory. *Cell* **127**, 49–58 (2006).
2. Walsh, M. J., Dodd, J. E. & Hautbergue, G. M. Ribosome-inactivating proteins: potent poisons and molecular tools. *Virulence* **4**, 774–784 (2013).
3. Puri, M., Kaur, I., Perugini, M. A. & Gupta, R. C. Ribosome-inactivating proteins: current status and biomedical applications. *Drug Discov. Today* **17**, 774–783 (2012).
4. Endo, Y. & Tsurugi, K. The RNA N-glycosidase activity of ricin A-chain. *Nucleic Acids Symp. Ser.* 139–142 (1988).
5. Hey, T. D., Hartley, M. & Walsh, T. A. Maize ribosome-inactivating protein (b-32). Homologs in related species, effects on maize ribosomes, and modulation of activity by pro-peptide deletions. *Plant Physiol.* **107**, 1323–1332 (1995).
6. Mak, A. N.-S. *et al.* Structure-function study of maize ribosome-inactivating protein: implications for the internal inactivation region and the sole glutamate in the active site. *Nucleic Acids Research* **35**, 6259–6267 (2007).
7. Schmidt, E. K., Clavarino, G., Ceppi, M. & Pierre, P. SUnSET, a nonradioactive method to monitor protein synthesis. *Nat. Methods* **6**, 275–277 (2009).
8. Dieterich, D. C. *et al.* In situ visualization and dynamics of newly synthesized proteins in rat hippocampal neurons. *Nat. Neurosci.* **13**, 897–905 (2010).
9. Tom Dieck, S. *et al.* Metabolic labeling with noncanonical amino acids and visualization by chemoselective fluorescent tagging. *Curr Protoc Cell Biol* **Chapter 7**, Unit7.11 (2012).
10. Davis, H. P. & Squire, L. R. Protein synthesis and memory: a review. *Psychol Bull* **96**, 518–559 (1984).
11. Ho, V. M., Lee, J.-A. & Martin, K. C. The cell biology of synaptic plasticity. *Science* **334**, 623–628 (2011).
12. Govindarajan, A., Israely, I., Huang, S.-Y. & Tonegawa, S. The dendritic branch is the preferred integrative unit for protein synthesis-dependent LTP. *Neuron* **69**, 132–146 (2011).
13. Cajigas, I. J., Will, T. & Schuman, E. M. Protein homeostasis and synaptic plasticity. *EMBO J.* **29**, 2746–2752 (2010).
14. Aakalu, G., Smith, W. B., Nguyen, N., Jiang, C. & Schuman, E. M. Dynamic visualization of local protein synthesis in hippocampal neurons. *Neuron* **30**, 489–502 (2001).
15. Atasoy, D., Aponte, Y., Su, H. H. & Sternson, S. M. A FLEX switch targets Channelrhodopsin-2 to multiple cell types for imaging and long-range circuit mapping. *J Neurosci* **28**, 7025–7030 (2008).
16. Woodhead, G. J., Mutch, C. A., Olson, E. C. & Chenn, A. Cell-autonomous beta-catenin signaling regulates cortical precursor proliferation. *J Neurosci* **26**, 12620–12630 (2006).
17. Link, A. J., Vink, M. K. S. & Tirrell, D. A. Preparation of the functionalizable methionine surrogate azidohomoalanine via copper-catalyzed diazo transfer. *Nat Protoc* **2**, 1879–1883 (2007).
18. Matsuzaki, M., Honkura, N., Ellis-Davies, G. C. R. & Kasai, H. Structural basis of long-term potentiation in single dendritic spines. *Nature* **429**, 761–766 (2004).
19. Taylor, J. R. *An Introduction to Error Analysis*. (Sterling Publishing Company, 1997).

Acknowledgments

We thank N. Fuerst, I. Bartnik and A. Staab for the preparation of cultured hippocampal neurons. We thank M. Lauterbach for the MATLAB script used to analyze spine-head volumes and we thank P. C. Shaw and C. Hanus for plasmids used in this study. E.M.S is funded by the Max Planck Society; This project has received funding from the European Research Council (ERC) under the European Union's Horizon 2020 research and innovation program (grant agreement No 743216).

Author contributions

M.H.: designed, conducted and analyzed experiments and edited the manuscript.
C.G.: designed, conducted and analyzed experiments and edited the manuscript.
V.R.: designed, conducted and analyzed the spine plasticity experiments and edited the manuscript.
A.B.: designed and conducted experiments and edited the manuscript.
E.M.S.: designed experiments and wrote the manuscript.

Competing interests

The authors declare no competing financial interests.

Materials & Correspondence

Correspondence to Erin M. Schuman.

Material and Methods

Cell Culture

Dissociated rat hippocampal neurons were prepared from P0-1 day-old rat pups as previously described¹⁴. Neurons were plated onto poly-d-lysine coated glass-bottom Petri dishes (MatTek) and cultured in neuronal growth medium (NGM, Neurobasal-A supplemented with B27 and GlutaMAX). The cultures were maintained in a humidified incubator at 37°C and 5% CO₂. HeLa cells were maintained in Dulbecco's modified Eagle's medium (DMEM, Invitrogen) supplemented with 10% FCS at 37°C in a 5% CO₂ atmosphere. **Once cells reached a confluency of 70% they were passaged.** Only cells that were passaged less than 10 times were used for experiments.

Transient transfection of hippocampal neurons or HeLa cells

Primary hippocampal neurons were transfected at DIV 11 using CombiMag following the manufacturer's recommendations. Experiments were performed at least 12 hrs post-transfection to guarantee sufficient expression of the constructs. HeLa cells, at 50% confluency, were transfected with Lipofectamin 2000 according to the manufacturer's guidelines. The inducible expression system TetOn3G was purchased from Takara Bio – Clontech (#631337). **Additional plasmids used in this study were gifted by P. C. Shaw, C. Hanus, S. Sternson¹⁵ (Addgene #18925), J. M. Wilson (Addgene # 105558) and A. Chenn¹⁶ (Addgene # 26646). Cloning was performed using Gibson Cloning.**

Dual, triple or quadruple transfections were performed with the following plasmids:

pCMV-TetOn3G + pTRE3G-Bi-ProRIP/ α -Chain/ β -Chain + pCMV-AcGFP-N1

pCMV-TetOn3G + pTRE3G-Bi-gePSI-pCMV-AcGFP

pCAMKIIa-TetOn3G + pTRE3G-Bi-gePSI-pCamk2a-AcGFP

pGFAP-TetOn3G + pTRE3G-Bi-gePSI-pGFAP-AcGFP

pCMV-FLEX_(inverted)-TetOn3G-3xHA-FLEX_(inverted) + pTRE3G-Bi-gePSI-pCMV-AcGFP + pCAG-Cre-IRES2-eGFP (Addgene #26646)

pCMV-FLEX_(inverted)-TetOn3G-3xHA-FLEX_(inverted) + pTRE3G-Bi-gePSI + pCamKII-Cre (Addgene #105558) + pCamkII-AcGFP

In each of the transfections, a 1:4 ratio between the activator plasmid (TetOn3G) and the responder plasmid (pTRE3G-Bi) was used. **The β -chain of gePSI is C-terminally fused to a murine ornithine decarboxylase (ODC36) degron.**

Doxycycline hyclate (dox) treatment

Doxycycline hyclate (Sigma-Aldrich/Merck, D9891) was dissolved in H₂O to yield a 1 mg/ml stock solution. Dox was added to the growth medium of transfected cells to a final working concentration of 1 μ g/ml to induce gePSI expression (unless otherwise stated). For the protein synthesis recovery experiments 10 ng/ml was used, neurons were washed three times with NGM and replaced with their growth medium that had been saved prior to dox treatment.

Fluorescent non-canonical amino acid tagging (FUNCAT)

FUNCAT was performed as previously described^{8,9} with the following modification: a biotin-alkyne (Acetylene-PEG4-Biotin, Jena Bioscience) was used as a tag in the copper-catalyzed [3+2] azide-alkyne cycloaddition (CuAAC) click reaction. Hippocampal neurons were incubated in methionine-free Neurobasal-A medium (custom-made by Life Technologies) supplemented with 4 mM AHA (prepared as described in¹⁷) for 1.5 hrs. Cells were washed two times with PBS-MC (1x PBS, pH 7.4, 1 mM MgCl₂, 0.1 mM CaCl₂) and fixed for 20 min in PFA-sucrose (4% paraformaldehyde, 4% sucrose in PBS-MC) at room temperature. Cells were washed with 1x PBS, permeabilized with 0.5% Triton X-100 in 1x PBS, pH 7.4, for 15 min and blocked with blocking buffer (4% goat serum in 1x PBS) for 1 hr. Cells were equilibrated to optimal click conditions by washes with 1x PBS, pH 7.8. After the click reaction, cells were incubated with primary antibodies (anti-MAP2 (SySy, 188004, 1:1000), anti-biotin (Cell Signaling, 5597, 1:2000) in blocking buffer overnight at 4°C. Secondary antibodies were incubated in blocking buffer for 45 min at room temperature.

Immunocytochemistry and puromycylation

Nascent proteins were labeled by incubating cells with puromycin (stock solution 50 mg/ml in H₂O; Sigma-Aldrich/Merck, P8833) at a final concentration of 3 μ M for 10 min in full medium at 37°C in a humidified atmosphere with 5% CO₂. Cells were then rinsed in 1x PBS and fixed for 20 min in PFA (4% paraformaldehyde in 1x PBS), permeabilized with 0.5% Triton X-100 in 1x PBS supplemented with 4% goat serum, for 15 min and blocked with blocking buffer (4% goat serum in 1x PBS) for 1 hr. Primary antibodies (anti-MAP2 (SySy, 188004, 1:1000), anti-puromycin (Kerafast, EQ0001, 1:2000)) were incubated in blocking buffer overnight at 4°C. Secondary

antibodies (ThermoFisher, A11030, 1:1000; Jackson IR, 106-475-003, DyLight 405, 1:500) were incubated in blocking buffer for 45 min at room temperature.

High-Resolution *in situ* hybridization

In situ hybridization was performed using the Quantigene ViewRNA ISH Cell Assay for Fluorescence with probes targeting the coding sequence of Camk2a (VC6-11639), GFAP (VC6-11478) or gePSI (α -Chain: VPWCWCK (type 6); β -Chain: VPXGPWH (type 1)). The manufacturer's protocol was applied with the following modifications: Cells were fixed for 20 min at room temperature using a 4% paraformaldehyde solution (4% paraformaldehyde, 5.4% glucose, 0.01 M sodium metaperiodate, in lysine-phosphate buffer). The Proteinase K treatment was omitted in order to preserve the integrity of the cells. After completing the *in situ* hybridization, cells were washed with 1x PBS and incubated in blocking buffer (4% goat serum in 1x PBS) for 1 hr. Nascent proteins and neuronal morphology was stained as described above.

Cell health assays

To assess cell health two assays were used:

The propidium iodide (PI) exclusion assay was performed by incubating cells in full medium with 1 μ l/ml PI (stock solution 1 mg/ml in H₂O; invitrogen/Thermo Fisher Scientific, P1304MP) and 20 μ M Hoechst 33342 (stock solution 20 mg/ml in H₂O; Sigma-Aldrich/Merck, B2261) for 10 min at 37°C in a humidified atmosphere with 5% CO₂. Cells were then transferred microscope (pre-heated chamber at 37°C) for live imaging. For the positive control, cells were treated with a final concentration of 10 mM H₂O₂ (stock solution 27% H₂O₂; Alfa Aesar, L13235) for 1h or 24h in full medium prior to PI/Hoechst staining.

The apoptosis assay 'Click-iT™ TUNEL Alexa Fluor™ 647 Imaging Assay' from ThermoFisher Scientific was used according to the manufacturer's protocol. For the positive control, cells were treated with DNase I solution for 30 min after fixation as indicated in the protocol.

Imaging and image analysis

Fluorescence imaging was performed with a LSM780 or LSM880 laser scanning confocal microscope (Zeiss) with x20 air objective (Plan Apochromat 20x/0.8 M27) or x40 oil objective (Plan Apochromat 40x/1.4 oil DIC M27) with appropriate excitation

laser lines and spectral detection windows. Images were acquired in 16-bit mode as z-stacks, covering the entire thickness of the cell, with 1024x1024- or 2048x2048-pixel image resolution. Laser power and detector gain were adjusted to ensure a good dynamic range, without saturating pixels. Imaging conditions were held constant within an experiment. For image analysis the raw images were split into single-channel images and maximum-intensity projections were created (Zeiss – Zen Black). To quantify the nascent protein signal for individual cells the cell body (soma for neurons) was manually traced to create a mask using the MAP2- and GFP-channel, the traced masks were then used in the ‘metabolic labeling’-channel and the mean intensity within the mask was measured (NIH-ImageJ). In order to correct for technical deviations (e.g. small differences in puro incubation times), the puro-signal of transfected cells was normalized to the mean puro-signal of a maximum of 10 untransfected, neighboring cells.

All live imaging experiments were performed at a temperature of 37 °C in modified E4 imaging buffer containing (in mM) 120 NaCl, 3 KCl, 10 HEPES (buffered to pH 7.4), 4 CaCl₂ (lacking MgCl₂) and 10 Glucose. Live cell imaging was performed using an inverted spinning disk confocal microscope (3i imaging systems; model CSU-X1) using the Slidebook 5.5 software. For glutamate uncaging experiments, images were acquired with a Plan-Apochromat 63x/1.4 Oil DIC objective at laser powers 1.1 mW (488 nm) and 0.8 mW (561 nm) using an Evolve 512 camera (Photometrics). 488 nm excitation and 525/30 nm emission filters were used for GCaMP6s; 561 nm excitation and 617/73 nm emission filters were used for PSD95-mCherry fluorescence. Images were analyzed using ImageJ, unless specified otherwise. OriginPro 2017 was used for data analysis, statistical testing and plotting graphs.

Uncaging and spine-head volume measurements

Neurons were transfected with GCaMP6s, PSD95-mCherry, pCMV Tet3G and pTRE3G-Bi-gePSI plasmid constructs. The absence of the pTRE3G-Bi-gePSI construct was used as control. Neurons were either treated with dox for 4 hours (for gePSI-induction) prior to the imaging, or untreated (control). Both gePSI-induced and untreated control neurons were identified by changes in GCaMP6s fluorescence corresponding to calcium transients in dendrites and spines. PSD95-mCherry fluorescence was used to identify spines for glutamate uncaging. Before glutamate uncaging, neuronal media was replaced with 1 μM TTX (Citrate salt, 2 mM stock

made in water), 50 μM Forskolin (Tocris Bioscience, 100 mM stock made in DMSO), 2 mM 4-Methoxy-7-nitroindolinyI-caged-L-glutamate (MNI caged glutamate) (Tocris Bioscience, 100 mM stock made in E4 buffer) in modified E4 buffer. Glutamate uncaging was performed using a multiphoton-laser 720 nm (Chameleon, Coherent) and a Pockels cell (Conoptics) for controlling the uncaging pulses. Spines that were at least 50 μm away from the cell body were chosen for uncaging experiments. To test a spine's response to an uncaging pulse, an uncaging spot ($\sim 2 \mu\text{m}^2$) close to a spine head was selected and two to three uncaging pulses at 10 ms pulse duration per pixel and 2.5 mW power were given and the spine was checked for spine-specific calcium transients. For synaptic transmission experiments an uncaging protocol of 30 uncaging pulses at 1 Hz with 10 ms pulse duration per pixel was used. For plasticity experiments, an uncaging protocol of 60 uncaging pulses at 0.5 Hz with 10 ms pulse duration per pixel, at 2.5 mW power was used. Images were acquired every 10 min for up to 55 min. For analysis of spine morphology, we used a custom-written Matlab script. Ten images from each time point were averaged and a line crossing the center of the spine-head was drawn. The fluorescence intensity measured along the line was fit to a Gaussian to obtain the full width at half maximum—defined as the spine-head diameter¹⁸. Spine-head diameter was converted to spine-head volume, under the assumption that the spine-head is spherical. The uncertainty of the spine-head diameter measurement was determined from standard error of the mean and was converted to the uncertainty of the spine-head volume by standard error propagation¹⁹.

Sample size choice and statistics

Sample size choice was determined as follows: within one replicate the maximum number of culture dishes was limited to 12 to ensure consistent experimental procedure for all dishes. The experimenter selected the transfected cells in the GFP-channel blind to the 'metabolic-labeling'-channel (not blind to the condition) and all or at least 20 transfected cells in a dish were imaged. Unless otherwise stated, all experiments were repeated with dishes originating from two independent cell preparations. Within one experiment at least 2 dishes were used per condition. The experiments in supplementary figure 2-4 were performed with multiple dishes originating from a single neuronal preparation (prepared from ~ 10 P0-1 rat pups). The "n" in the figure legends depict the number of cells imaged per condition. For quantification and testing of statistical significance, data are displayed as combined

graphs from multiple experiments. For all data sets, the Pearson omnibus normality test was applied to test for normal distribution. If normality was proven, Student's, unpaired t-test (for two groups) was applied. For non-normally distributed data sets, the Mann-Whitney U test (for two groups) or Kruskal-Wallis test was applied (for three or more groups). An F-test was applied to compare variances before Student's t-test. For multiple-comparison analysis, Dunn's test of multiple comparisons was applied.

Figure legends

Figure 1. Design and function of the gePSI

a-c, The working principle. **a**, the gePSI renders ribosomes inoperative by depurinating adenine-4324 on the sarcin/ricin loop of the 28s rRNA. **b**, The TetOn-System enables the temporal and cell type-specific expression of gePSI upon doxycycline (dox) administration. **In the presence of dox the cell type-specific expression of the gePSI is enabled, shutting off protein synthesis.** **c**, Schematic of the transfected plasmids: (i) ProRIP and (ii) the gePSI (see also Fig S1a). Addition of dox together with expression of the Tet-On 3G protein leads to expression of either construct. **d-e**, Representative fluorescence images of hippocampal neurons transfected with the ProRIP (**d**) or the gePSI (**e**). Nascent protein signal is shown in red, anti-MAP2 immunostaining to visualize neuronal morphology is shown in blue. GFP (green) or dashed white outlines indicate transfected neurons. **The following plasmids were co-transfected in these experiments: pCMV-Tet3G + pTRE3G-ProRIP + pCMV-AcGFP or pCMV-Tet3G + pTRE3G-Bi-gePSI-pCMV-AcGFP.** Scale bar = 20 μm . **f-g**, Analysis of (**d-e**). Each dot represents the nascent protein signal intensity from one neuron normalized to the mean nascent protein signal of neighboring, untransfected neurons. From left to right:
n = 239, 46, 65; mean = 1, 0.34, 0.19; sd = 0.31, 0.29, 0.06; **** p < 0.0001; Kruskal-Wallis test followed by Dunn's multiple comparison test (**f**). From left to right:
n = 369, 82, 86; mean = 1, 1.1, 0.21; sd = 0.34, 0.39, 0.1; **** p < 0.0001; Kruskal-Wallis test followed by Dunn's multiple comparison test (**g**).

Figure 2. Temporally – resolved protein synthesis inhibition

a-b, On-kinetics of gePSI in neurons. **a**, Schematic (top) and analysis (bottom) of nascent protein signal after 0, 0.5, 1, 2 and 4h of dox incubation; protein synthesis was measured for the last 10 min of each dox incubation period. Each dot represents the nascent protein signal intensity from one neuron normalized to the mean nascent protein signal of neighboring, untransfected neurons. From left to right: n = 19, 20, 18, 20, 19; mean = 1.03, 0.97, 0.9, 0.2, 0.18; sd = 0.27, 0.27, 0.39, 0.17, 0.04; **** p < 0.0001; Kruskal-Wallis test followed by Dunn's multiple comparison test. **In these experiments and those shown below (b-d), the following plasmids were co-transfected: pCMV-Tet3G + pTRE3G-Bi-gePSI-pCMV-AcGFP.** **b**, Schematic (top) and analysis (bottom) of nascent protein signal after 0, 0.5, 1 and 2h of dox incubation, followed by a chase without dox up to 4h. Each dot represents the

nascent protein signal intensity from one neuron normalized to the mean nascent protein signal of neighboring, untransfected neurons. From left to right: $n = 59, 50, 41, 45$; mean = 1.1, 0.34, 0.3, 0.23; sd = 0.3, 0.28, 0.25, 0.15; **** $p < 0.0001$; Kruskal-Wallis test followed by Dunn's multiple comparison test. **c-d**, Reversibility of gePSI-mediated protein synthesis inhibition. **c**, Schematic (top) and representative images of hippocampal neurons transfected with gePSI (bottom). Nascent protein signal is shown in red. GFP (green) or dashed white outlines indicate transfected neurons. Images represent the time points indicated in the schematic. Scale bar = 20 μm . **d**, Analysis of (c). Each dot represents the nascent protein signal intensity from one neuron normalized to the mean nascent protein signal of neighboring, untransfected neurons. From left to right: $n = 115, 121, 115, 115, 100$; mean = 1.1, 0.26, 0.57, 0.86, 1; sd = 0.32, 0.23, 0.48, 0.54, 0.43; ns $p > 0.05$, ** $p < 0.01$, *** $p < 0.001$, **** $p < 0.0001$; Kruskal-Wallis test followed by Dunn's multiple comparison test.

Figure 3. gePSI induction does not perturb neuronal responses but prevents spine structural plasticity

a, Representative images of stimulated neurons without (no dox) and with (4h dox) gePSI induction. Nascent protein signal in red, anti-MAP2 in blue and GCaMP6 in green. The arrowheads indicate the 2p glutamate uncaging spots. The following plasmids were co-transfected in these experiments: pCMV-Tet3G + pTRE3G-Bi-gePSI + pCMV-GCaMP6s (a-c). Scale bar = 20 μm . **b**, Magnification of the uncaging spots in (a). Images show calcium signal 100 ms before, during (stim), and 100 / 500 ms after 2P glutamate uncaging. Scale bar = 2 μm . **c**, Analysis of calcium signal after gePSI induction (4h dox, red) and without gePSI induction (no dox, blue). Plotted is the mean change in calcium signal to 30x 2P uncaging events (delivered at 1 Hz) compared to the baseline calcium signal before stimulation. For analysis, the 5 frames following each uncaging event were averaged and the mean of the 30 events were compared between treatments. $n = 10, 12$; ns $p > 0.05$; Mann-Whitney U test. **d**, Schematic (top) of experiment and group analysis (bottom) of spine-head volumes after local glutamate uncaging. gePSI expression without dox induction (blue, solid line, $n = 21$ spines from 6 cells), dox administration with the isolated expression of Tet3G (blue, dashed line, $n = 14$ spines from 4 cells) or gePSI induction (red, solid line, $n = 15$ spines from 4 cells). Depicted are means \pm SEM. gePSI w/ dox compared to gePSI w/o dox: $p < 0.0005$; gePSI w/o dox compared to Tet3G w/ dox: $p = 0.5$;

One way ANOVA, Tukey test for mean comparisons. The following plasmids were co-transfected in these experiments: pCMV-Tet3G + pTRE3G-Bi-gePSI + pCMV-GCaMP6s + pCMV-PSD-95-mCherry (d-e). e, Representative images of stimulated spines (dashed white outline) with (4h dox) and without (no dox) gePSI induction; directly before (0 min) and 25 / 55 min after spine stimulation. The dot indicates the 2p glutamate uncaging spot. Scale bar = 2 μ m.

Figure 1 - Design and function of the gePSI

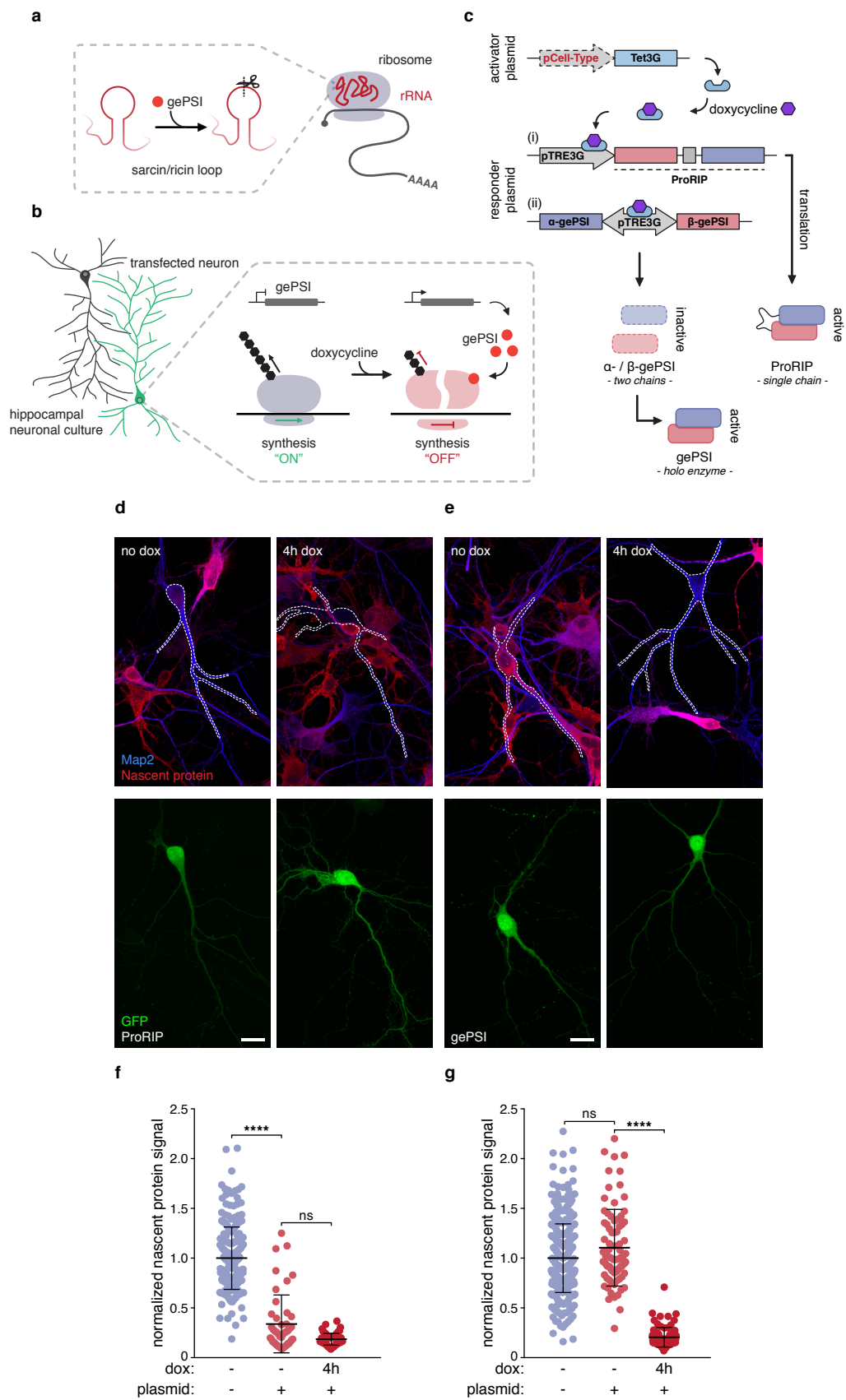


Figure 2 - Temporally - resolved protein synthesis inhibition

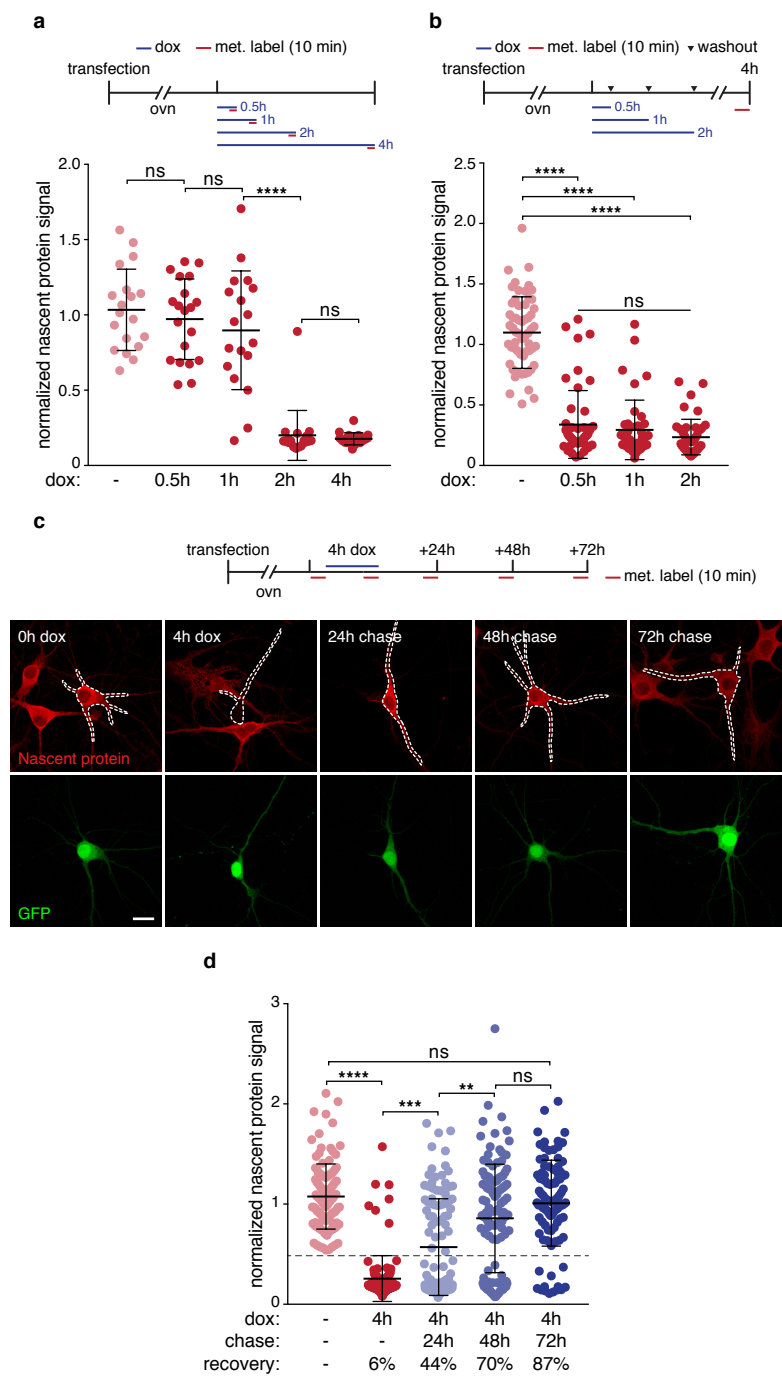


Figure 3 - gePSI induction does not perturb neuronal responses but prevents spine structural plasticity

